Journal of the Korean Magnetic Resonance Society **1999**, *3*, 60-70

NMR Structural Study of the 3′-T•G Mismatched DNA Decamer Duplex Containing the T-T (6-4) Adduct

Joon-Hwa Lee, Yun-Jeong Choi, and Byong-Seok Choi*

Department of Chemistry, Korea Advanced Institute of Science and Technology
373-1, Kusong-dong, Yusong-gu, Taejon 305-701
Received May 20, 1999

Abstract: The pyrimidine(6-4) pyrimidone photoproduct [(6-4) adduct] is one of the major photoproducts induced by UV irradiation of DNA and occurs at TpT sites. The (6-4) adduct is highly mutagenic and specific during translesion replication. The marked preference for insertion of A opposite the 5′-T and G opposite the 3′-T of the (6-4) adducts leads to a predominantly 3′-T→C transition with 85% replicating error rate. In order to obtain insight into the origin of 3'-T→C transition induced by the (6-4) adduct, we have performed one - and two-dimensional NMR experiment. The 3′-T of the (6-4) lesion forms the stable hydrogen bonding to the imino proton of an opposed G, which stabilizes the overall helix and diminishes the highly distorted conformation caused by the (6-4) lesion in the (6-4)/AA duplex. We proposed that the greater insertion of a G over an A opposite the 3′-T of the (6-4) lesion These results may account for the greater preference for the insertion of a G over an A opposite the 3′-T of the (6-4) lesion. Thus this insertion leads to the highly specific 3′-T→C mutation at the (6-4) lesion site.

INTRODUCTION

Ultraviolet (UV) light radiation damages DNA and leads to mutation and cancer.[1-4] The *cis-syn* cyclobutane pyrimidine dimer (*cis-syn* dimer) and (6-4) adduct are two major classes of UV-induced DNA photoproducts (Fig. 1A).[5-7] The *cis-syn* dimer and (6-4) adduct are produced directly by sunlight at relative rate of approximately 10:1.[7] The *cis-syn* dimer undergoes excision repair in vivo with a half life of 24 hours whereas the (6-4) adduct is repaired rapidly with a half life of 4 hours.[8] In vitro the *cis-syn* dimer is repaired about nine times slower than the (6-4) adduct by the *Escherichia coli* uvr(A)BC endonuclease.[9] DNA polymerase bypasses the *cis-syn* dimer and (6-4) adduct with relative rates of 1:0.006.[10] The

cis-syn dimer of TpT site is not mutagenic, whereas the (6-4) adduct is highly mutagenic. In *Escherichia coli* under stringent conditions, A residues were found to be incorporated opposite both T residues of *cis-syn* dimer with a frequency of 94%.[11] Likewise, A was incorporated opposite the 5'-T of the (6-4) adduct 95% of the time, but was incorporated opposite the 3'-T only 11% of the time, while G was incorporated 88% of the time.[12-14] The marked preference for insertion of A opposite the 5'-T and G opposite the 3'-T of the (6-4) adducts during DNA synthesis bypass leads to a predominantly 3'-T→C transition with 85% replicating error rate.[12-14] Although a model of possible hydrogen bonding interaction was proposed to explain the high mutability and specificity of the (6-4) adduct based on thermodynamic and base pairing studies,[15, 16] no structural study of DNA duplexes containing (6-4) adducts in mutated sequence context has been reported.

We have performed the NMR study of the DNA decamer duplex which contains the mismatched base pair between the 3'-T of the (6-4) adduct and an opposed G (designated by (6-4)/GA duplex, Fig. 1B), where the conformational influence of T6•G15 base pair in the (6-4)/GA duplex has been compared with that of T6•A15 base pair in the (6-4)/AA duplex which was established in the previous work.[17]

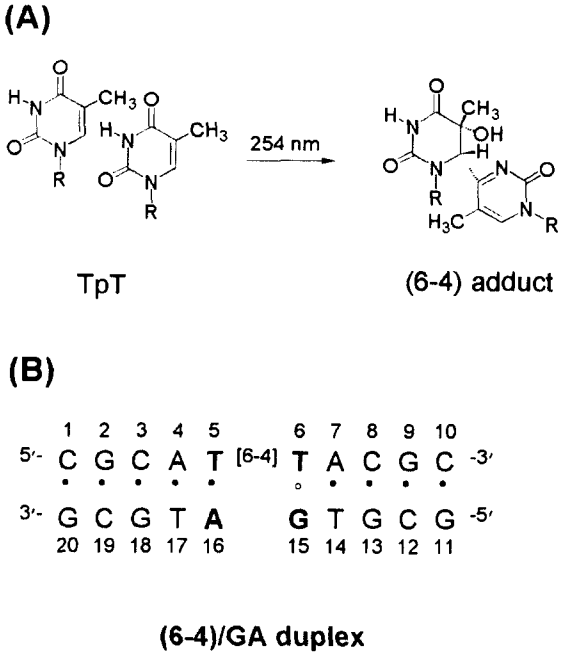

Fig. 1. (A) Chemical structure of the (6-4) adduct. (B) DNA sequence context of the (6-4)/GA duplex.

METHODS

Sample Preparation

The single-stranded oligonucleotides, d(CGCATTACGC) and d(GCGTGAT GCG) were synthesized by phosphoramidite method on a DNA synthesizer (Applied Biosystem, model 391). The crude 5′-dimethoxytritilated oligonucleotides were deprotected by treatment with concentrated ammonia for 12 hours at 55℃. The DNA products were purified by reverse-phase HPLC and desalted by Sephadex G-25 column.

The thymine (6-4) adduct was produced by irradiating the oligonucleotide, d(CGCATTACGC), in aqueous solution contained in large petri dish using a radiation reactor (New Southern England UV Products, model RPR-2000) equipped with twelve 35-W germicidal lamps (254-nm) for 6 hours. The average irradiating intensity was 80 J/m^{2}s. The temperature of the reactor chamber was maintained around 10℃ by purging with liquid nitrogen gas during irradiation. Irradiated samples were dried and fractionated using a preparative μ -Bondapak C-18 HPLC column with a 60-min 10-20% methanol gradient in 20 mM sodium phosphate buffer, pH 7.0, at a flow rate 2.5-ml/min. The (6-4) adduct, which was characterized by maximum absorption band at near 325-nm, was repurified by HPLC with a 60-min 10-20% methanol gradient in the previous buffer system and by Sephadex G-25 column. The (6-4)/GA duplex was prepared by dissolving the lesion-containing and complementary oligonucleotide strand (adjusted to a stoichiometric 1:1 ratio) in an aqueous solution containing 10mM sodium phosphate (pH 6.6) and 200 mM NaCl.

NMR Experiments

All NMR experiments were carried out using Bruker DMX-600 spectrometers. The data were processed using a Silicon Graphics workstation with the program *XWIN* and *FELIX 95.0*. The spectra were recorded within the temperature range of 1-25℃. For observation of the exchangeable protons, one-dimensional proton spectra in H_2O solution were collected with water suppression by a jump-and-return pulse.[18] The NOESY spectrum in H_2O solution at 1℃ was recorded using jump-and-return pulse sequence for the reading pulse with mixing times of 120 and 250 ms. The phase-sensitive NOESY spectra in D_2O solution were recorded with mixing times of 80, 160, and 300 ms using time-proportional phase incrementation at 1℃. The spectra were acquired with 2 K data-points in the t_2 dimension and 512 points in the t_1 dimension. The time-domain data were zero-filled in both directions to 4K×4K and multiplied with a phase-shifted squared-sine function before Fourier transformation.

RESULTS AND DISCUSSION

Resonance Assignment of the Exchangeable Protons

The one- and two-dimensional NMR data on the (6-4)/GA duplex in H_2O solution have been analyzed to elicit the base pairing and stacking in the vicinity of the (6-4) lesion. The NOESY spectra of the (6-4)/GA duplex in shown in Fig. 2, in which all imino protons were assigned following the standard analysis scheme of labile protons.[19] The H5 protons of all C residues exhibited NOEs to both the hydrogen-bonded and non-hydrogen-bonded amino protons. One amino proton of each C residue also exhibited an NOE to the other amino proton. The imino protons of all G•C base pairs were assigned by observing a set of NOE cross peaks from the C amino protons, which were assigned by intraresidue NOEs of H5↔NH_2, to the G imino proton on the opposed base (Fig. 2A). The imino protons of all T•A base pairs were assigned from NOEs between the T imino protons and the H2 protons on the opposite A residue. The H2 protons of adenine residues were assigned from intraresidue NOEs of H2↔H1'. The imino proton of G15 base-paired with the 3'-T of the (6-4) adduct residue was resonated at 10.30 ppm. NOE interaction of G15 imino proton with own amino proton indicated that the G15 residue had the unusual hydrogen bonding. The imino to imino NOE interactions of the (6-4)/GA duplex were observed at G2-NH↔G18-NH, G18-NH↔T17-NH, T14-NH↔G13-NH, and G13-NH↔G9-NH steps (Fig. 2B). The discontinuities or weakness in the sequential NOEs of imino to imino protons suggested a significant disturbance in the stacking interaction. The significantly weaker intensity of T17-NH↔G18NH than that of the (6-4)/AA duplex indicates that the 5'-side of the (6-4) lesion is destabilized than its 3'-side. The chemical shifts of all imino and the amino protons of all C residues were given in Table 1.

Exchange behavior of the imino protons

The temperature-dependent ^1H spectra of the imino protons of the (6-4)/GA duplex were presented in Fig. 3. Increasing temperature led to thermal denaturation of the double helical structure with the contaminant line broadening and eventual disappearance of the imino proton resonances, formerly involved in hydrogen bonding. The striking feature is the persistence of the imino proton signals of G15 as well as all other base pairs of the (6-4)/GA duplex up to 20℃, whereas all the imino proton resonances of the (6-4)/AA duplex were disappeared at 10℃.[20] This result indicates that the 3'-T•G base pairing of the (6-4) adduct contains the stable hydrogen bonding of the G15 imino proton and improves the overall helical stability than its 3'-T•A base pairing. This observation may have a significant correlation with the targeting of the 3'-T→C mutation predominantly to the (6-4) lesion.[12-15]

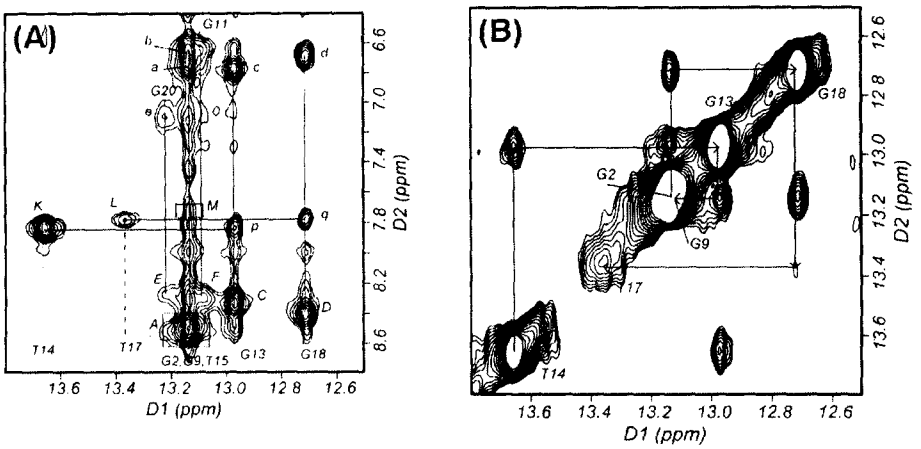

Fig. 2. Expanded NOESY (120-ms) contour plots of the (6-4)/GA duplex in H_2O buffer solution containing 10 mM sodium phosphate (pH 6.6) and 200 mM NaCl. (A) NOE cross peaks between the G-imino and C-amino protons of the G•C base pairs and those between T-imino and A-H2 protons of the T•A base pairs. (B) sequential connectivity between imino protons of the (n)- and (n+1)-base pairs.

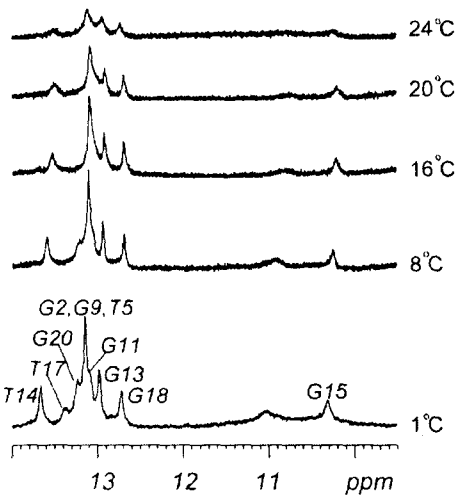

Fig. 3. Temperature dependence of the imino proton resonances of the ^{1}H-NMR spectra for the (6-4)/GA duplex in H_2O buffer solution. The experimental temperatures are shown on the right.

Table 1. Chemical shifts of proton resonances in the (6-4)/GA duplex.

Base	NH/NH_2	H2/H5/Me	H6/H8	H1′	H2′/H2″	H3′	H4′
C1	8.27/7.14	5.89	7.67	5.76	2.03/2.46	4.75	4.11
G2	13.14	-	8.01	5.92	2.70/2.76	5.02	4.41
C3	8.42/6.68	5.44	7.35	5.77	2.14/2.47	4.85	4.27
A4	-	7.77	8.29	6.40	2.83[1]	4.97	4.43
T5	13.14	1.26	4.75	5.54	0.94/1.86	4.75	3.90
T6	-	2.28	7.96	6.24	2.64/3.03	5.01	3.89
A7	-	7.83	8.45	6.35	2.82/3.00	5.09	4.48
C8	8.34/6.78	5.37	7.33	5.59	2.02/2.35	4.88	4.16
G9	13.15	-	7.89	5.98	2.61/2.75	5.01	4.40
C10	8.29/6.65	5.19	7.36	6.16	2.26/2.30	4.54	4.04
G11	13.09	-	8.00	6.00	2.67/2.83	4.90	4.33
C12	8.49/6.67	5.38	7.44	5.79	2.18/2.50	4.93	4.24
G13	12.98	-	8.01	6.02	2.70/2.83	5.04	4.43
T14	13.67	1.52	7.15	5.95	1.98/2.46	4.89	4.26
G15	10.30	-	7.76	5.46	2.22/2.35	4.93	4.18
A16	-	7.62	8.28	6.09	2.70/2.79	5.02	4.37
T17	13.37	1.46	7.23	5.69	2.17/2.39	4.83	4.19
G18	12.72	-	7.96	5.96	2.68[1]	5.03	4.44
C19	8.53/6.74	5.45	7.43	5.81	2.01/2.40	4.90	4.24
G20	13.23	-	7.99	6.20	2.41/2.70	4.74	4.24

[1] Two resonances have been overlapped.

Resonance Assignment of the Non-exchangeable Protons

The non-exchangeable proton assignment for the (6-4)/GA duplex was based on analysis of distance-connectivities in NOESY data sets and bond-connectivities in COSY-type data sets recorded at 1 ℃. The NOESY spectra were acquired with a variety of mixing times. First, cytosine base proton resonances were identified by their H5 and H6 cross peaks in both NOESY and DQF-COSY spectra (*data not shown*). And then, the assignment of base and sugar proton resonances followed from a standard sequential strategies.[19] An expanded portion of a 300-ms NOESY spectra were shown in Fig. 4. These contour plot outlined the sequential intra-strand NOE connectivities between the base H6/H8 and sugar H1′ protons. Standard sequential NOE connectivities in the (6-4) lesion strand were well observed from C1 to A4 and from T6 to C10 (Fig. 4A). The resonance of T5-H6 proton was upfield-shifted to H3′ region (4.75 ppm, Fig. 4C), because of the saturation of the 5-6 double bond of the T5 base by forming the (6-4) adduct. No NOE was observed between A4-H1′ and T5-H6 and between T5-H1′ and T6-H1, indicating a substantial structural change in the vicinity of the (6-4) lesion. All sequential NOEs of the complementary strand were also observed (Fig. 4B). The chemical shifts of non-exchangeable protons of the (6-4)/GA duplex were listed in Table 1.

The base proton assignments were confirmed in the base to H2′/H2″ and base to H3′ regions of NOESY contour plot (*data not shown*). These regions of the NOESY spectrum were also used for initial assignments of the H2′/H2″ and H3′ protons. The assignments of the methyl groups were confirmed by the NOE cross peaks between methyl protons and own and (*n-1*) neighboring base protons (*data not shown*). All H2 protons of A4, A7, and A15 residues showed NOE interactions, with H1′ of their 3′-side and own residue, and interstrand NOE cross peaks were observed for A4-H2↔T17-H1′, A7-H2↔T14-H1′, and A16-H2↔T5H1′ (Fig. 4D) which were often associated with narrow minor group in the bending geometry, as was the case for the (6-4)/AA duplex.[17] Cross peaks involving the H2 resonances are important for constraining the width of the minor groove, in this case , for assessing base-pairing surrounding the dimer site.

NOEs between A7-H8 and most sugar protons of T6 residues, which were absent in the (6-4)/AA duplex,[20] were detected (*data not shown*). Likewise, the NOE cross peak between A7-H8 and T6-H1′ was stronger than that in the (6-4)/AA duplex (Fig. 4A). This observation suggests that the structural distortion at the 3′-side of the (6-4) lesion site is less than that in the (6-4)/AA duplex.

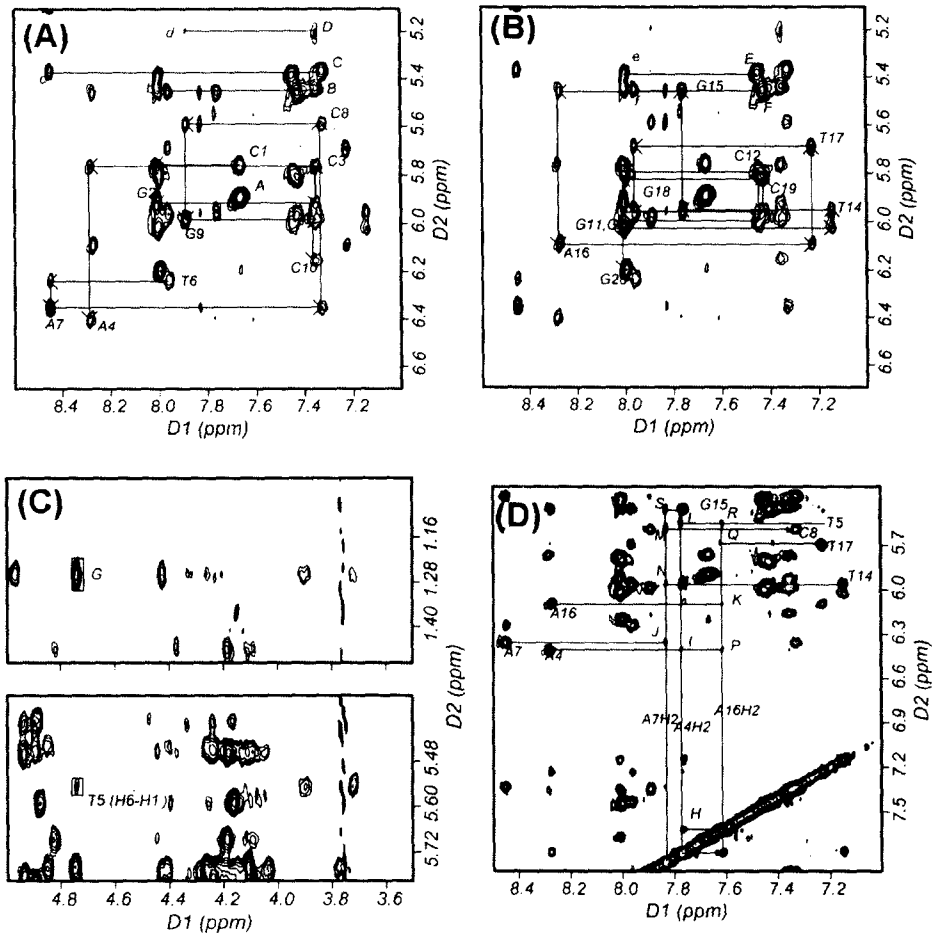

Fig. 4. Expanded NOESY (300-ms mixing time) contour plots of the (6-4)/GA duplex in D_2O buffer at 1℃. (A) A typical region (base to H1′ protons) in the sequential NOE connectivity of the (6-4) lesion strand (B) the complementary strand. NOE cross peaks A to F for C-H5↔C-H6 were assigned as follows: A, C1; B, C3; C, C8; D, C10; E, C12; F, C19. NOE cross peaks b to f were assigned as follows: b, C3-H5↔G2-H8; c, C8-H5↔A7-H8; d, C10-H5↔G9-H8; e, C12-H5↔G11-H8; f, C19-H5↔ G18-H8. (C) The resonance of T5-H6 was upfield-shifted to 4.75 ppm. Cross peak H is NOE between T5-H6 and T5-methyl protons. (D) NOE interaction (cross peaks of I to S) of A-H2 protons with neighboring A-H2 and sugar H1′ protons.

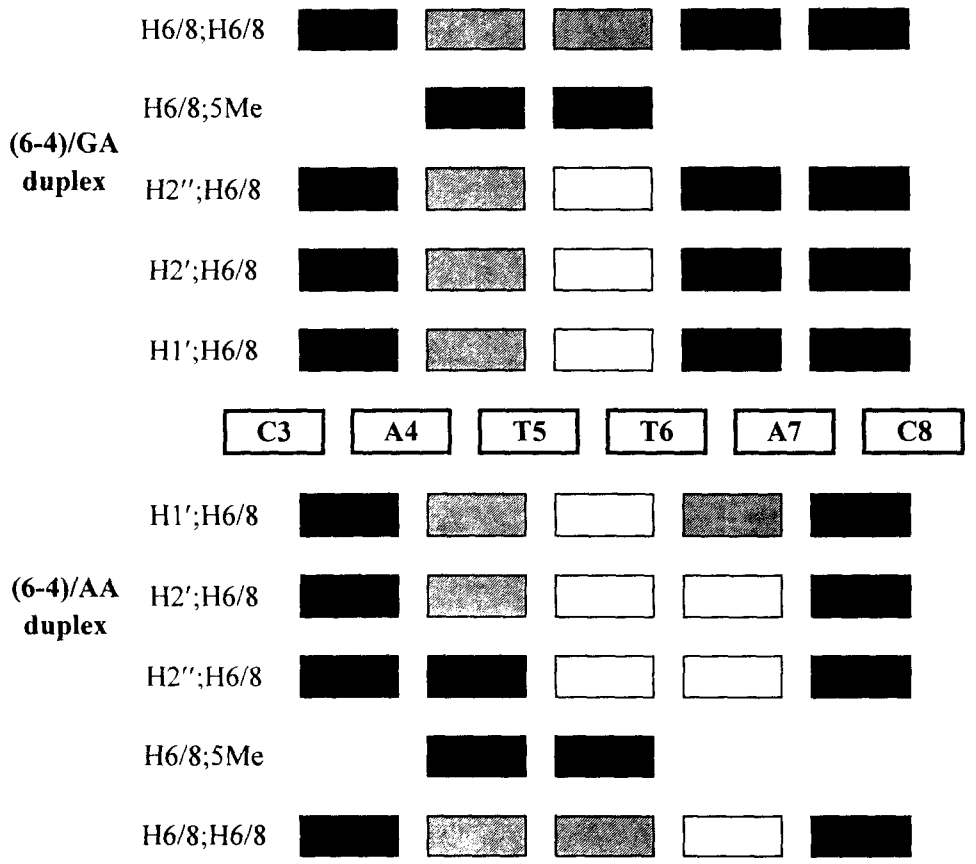

Fig. 5. Summary of the internucleotide cross peak intensities of photomodified strands observed in the NOESY spectra of the (6-4)/GA and the (6-4)/AA duplexes. Cross peaks of readily observable intensity are indicated by dark solid boxes, those of very week intensity by bright solid boxes, and those which were unobservable by blank boxes.

Biological Implication

The most striking conformational feature concerns the hydrogen bonding in the mismatched 3′-T•G base pair of the (6-4) adduct which is confirmed by the persistence of the imino proton signals of G15 as well as all other base pairs of duplex (6-4)/GA up to 20℃ (Fig. 3). The T6 can form hydrogen bonding with the imino proton of the opposite G15 residue, while there is no hydrogen bonding between the amino proton of A15 residue and 3′-T of the (6-4)/AA duplex.[20] The most straightforward interpretation of this observation is that

the mismatched 3'-T•G base pair dramatically increases the overall stability, which is in agreement with recent thermodynamics study.[16] This high stability might facilitate the misincorporation of G instead of A as the countpart of its 3'-T during the translesion replication.

The distortions in DNA helical conformation, which were induced by the formation of the (6-4) adduct in the (6-4)/AA duplex, are reduced significantly by its corresponding 3'-T•G base pairing in the (6-4)/GA duplex. This structural feature is consistent with the significant observation of the sequential NOEs between T6 sugar and A7-H8 protons which were absent in the (6-4)/AA duplex[17] (Fig. 5).

In summary, using NMR experiment, we have demonstrated the structural features unique to the 3'-T•G base pair of the (6-4)/GA duplex in solution. The 3'-T of the (6-4) lesion forms the stable hydrogen bonding with imino proton of an opposed G. This stable hydrogen bonding dramatically stabilizes the overall helix and restores the highly distorted conformation of the (6-4) lesion in the (6-4)/AA duplex to the typical B-form-like structure. This demonstrates that the greater stability of G over A opposite 3'-T of the (6-4) lesion may facilitate the misincorporation of G instead of A during the replication process and lead s to the highly specific 3'-T→C mutation at this site.

Acknowledgements

This work was supported by the Korea Science and Engineering Foundation(Grant 981-0304-024-2) and the Korea Science and Engineering Foundation through the Center for Molecular Catalysis at Seoul National University.

REFERENCES

1. D. E. Brash, *Photochem. Photobiol.* **48**, 59, (1988).
2. D. L. Mitchel, *Photochem. Photobiol.* **48**, 51, (1988).
3. H. N. Ananthaswamy, W. E. Pierceall, *Photochem. Photobiol.* **52**, 1119, (1990).
4. D. E. Brash, J. A. Rudolph, J. A. Simon, A. Lin, G. J. McKenna, H. P. Baden, A. J. Halperin, J. Potén, *Proc. Natl. Acad. Sci. USA* **88**, 10124, (1991).
5. D. L. Mitchell, R. S. Nairn, *Photochem. Photobiol.* **49**, 805, (1989).
6. S. Y. Wang, (ed.) "Photochemistry and Photobiology of Nucleic Acids", Vol. I and II, Academic press, Inc., New York, (1976).
7. J. E. Cleaver, *Nature*, **218**, 652, (1968).
8. G. P. Pfeifer, *Photochem. Photobiol.* **65**, 270, (1997).
9. D. L. Svoboda, C. A. Smith, J. S. Taylor, A. Sancar, *J. Biol. Chem.* **268**, 10694, (1995).

10. C. A. Smith, J. Baeten, J. S. Taylor, *PJ. Biol. Chem.* **273**, 21933, (1998).
11. S. K. Banerjee, R. B. Christensen, C. W. Lawrence, J. E. LeClerc, *Proc. Natl. Acad. Sci. USA* **85**, 8141, (1988).
12 J. E. LeClerc, A. Borden, C. W. Lawrence, *Proc. Natl. Acad. Sci. USA* **88**, 9685, (1991).
13. P. E. M. Gibbs, A. Borden, C. W. Lawrence, *Nucleic Acids Res.* **23**, 1919, (1995).
14. A. Gentil, F. Le Page, A. Margot, C. W. Lawrence, A. Borden, A. Sarasin, *Nucleic Acids Res.* **24**, 1837, (1996).
15. C. A. Smith, M. Wang, N. Jiang, L. Che, X. Zhao, J. -S. Taylor, *Biochemistry* **35**, 4146, (1996).
16. Y. Fujiwara, S. Iwai, *Biochemistry* **36**, 1544, (1997).
17. J. K. Kim, B. S. Choi, *Eur. J. Biochem.* **228**, 849, (1995).
18. P. Plateau and M. Guéron, *J. Am. Chem. Soc.* **104**, 7310, (1982).
19. K. Wüthrich, "NMR of Proteins and Nucleic Acids", Wiley, New York, (1986).
20. G. S. Hwang, J. K. Kim, B. S. Choi, *Eur. J. Biochem.* **235**, 359, (1996).